SPREADING PHENOMENA IN INTEGRODIFFERENCE EQUATIONS WITH NON-MONOTONE GROWTH FUNCTIONS*

ADÈLE BOURGEOIS†, VICTOR LEBLANC†, AND FRITHJOF LUTSCHER†‡

Abstract. Integrodifference equations are discrete-time cousins of reaction-diffusion equations. Like their continuous-time counterparts, they are used to model spreading phenomena in ecology and other sciences. Unlike their continuous-time counterparts, even scalar integrodifference equations can exhibit non-monotone dynamics. Few authors studied the existence of spreading speeds and travelling waves in the non-monotone case; previous numerical simulations indicated the existence of travelling two-cycles. Our numerical observations indicate the presence of several spreading speeds and multiple travelling wave profiles in these equations. We generalize the concept of a spreading speed to encompass this situation and prove the existence of such generalized spreading speeds and associated travelling waves in the corresponding second-iterate operator. Our numerical simulations let us conjecture that these spreading speeds could be linearly determined. We prove the existence of bistable travelling waves in a related second-iterate operator. We relate our results to the existence of stacked waves and to dynamical stabilization.

Key words. integrodifference equation, non-monotone growth function, asymptotic spreading speed, travelling wave, stacked wave

AMS subject classifications. 37L15, 39A11, 92D40, 92D25

1. Introduction.

Spreading processes are ubiquitous phenomena in science that arise in areas as diverse as flame fronts, action potentials, or biological invasions. The two most important questions in this context ask how fast the quantity of interest propagates and what shape it forms. Accordingly, there is a vast body of literature on mathematical modelling and analysis of spreading phenomena, specifically on the corresponding mathematical concepts of the 'asymptotic spreading speed' [30] and the profile of a 'travelling wave' [12]. Depending on the phenomenon of interest, the time and space variables in the mathematical model may be chosen discrete or continuous. In this paper, we work with a spatially continuous, time-discrete model, known as 'integrodifference equation' [14] or 'integral recursion' [30].

Integrodifference equations are particularly well suited to model the dynamics of a biological population with discrete, non-overlapping generations and temporally separated growth and dispersal phases; a pattern that many plant and insect populations exhibit [14]. The quantity of interest is a one-dimensional density representing the population, whose value in generation t (in time) and point x (in space) is denoted by $N_t(x)$. The growth phase, during which individuals are spatially stationary, is modelled by a growth function F. The dispersal phase is described by a 'dispersal kernel' K, which is the probability density function of the signed distances that an individual disperses [22]. The 'next generation operator' Q that maps the density at time t to the density at time $t+1$ is given by the composition of growth and dispersal as the convolution integral operator

$$N_{t+1}(x) = Q[N_t](x) = [K * F(N_t)](x) = \int_{\mathbb{R}} K(x-y)F(N_t(y))dy. \tag{1}$$

*Submitted to the editors April 2017.

Funding: This work was funded by the Natural Sciences and Engineering Research Council of Canada (RGPIN-2016-04318 and RGPIN-2016-04795)

†Department of Mathematics and Statistics, University of Ottawa, Ottawa, ON, Canada (abour115@uottawa.ca, vleblanc@uottawa.ca, flutsche@uottawa.ca).

‡Department of Biology, University of Ottawa, Ottawa, ON, Canada

Unless otherwise noted, integrals in this work will be over the entire real line, and we will drop the symbol $\mathbb{R}$ from the integral if no confusion can arise. The symbol $*$ will denote the convolution of two functions over the real line as defined in (1).

Integrodifference equations have been used quite successfully to model biological invasions [5, 8, 13], most commonly by studying properties of travelling wave solutions, i.e. solutions of (1) of the form $N_t(x) = W(x - ct)$, where W is the spatial profile and c is the speed of the invasion. While the existence and shape of such a profile depend on properties of both F and K, we focus on the influence of the growth function. We list the standard requirements on K in the next section.

In the simplest biologically relevant application, the non-spatial, one-dimensional map $N \mapsto F(N)$ is monotone increasing, concave down, and has two fixed points: $N^* = 0$ is linearly unstable and $N^* = 1$ is globally asymptotically stable. We can and shall always scale a positive fixed point to equal 1. The Beverton-Holt function

$$F(N) = \frac{RN}{1 + (R-1)N} \tag{2}$$

with $R > 1$ has these properties. Then there is a minimal speed c^*, such that the spatial model (1) has constant-speed, monotone travelling waves that connect the two fixed points of the non-spatial map for all $c \geq c^*$ [30]. In contrast, the Ricker function

$$F(N) = N \exp(r(1 - N)) \tag{3}$$

is not monotone but may still have an unstable fixed point at $N = 0$ and a stable point at $N = 1$, provided $0 < r < 2$. In this case, there is again a minimal speed c^*, and for each $c \geq c^*$ one can observe numerically a non-monotone travelling wave for the integrodifference equation (1), connecting the two fixed points [12]. The existence of such a travelling wave was proved in [10, 15, 33]. The positive fixed point of the Ricker function can lose stability via a flip bifurcation where a stable two-cycle emerges. In fact, the dynamics of the Ricker function are qualitatively the same as those of the famous discrete logistic function

$$F(N) = (1 + r)N - rN^2. \tag{4}$$

If the growth function exhibits a stable two-cycle or more complex behaviour, it is natural to ask whether the spatial dynamics of (1) are similarly complex. In some cases, one can still prove the existence of a travelling wave profile [10, 15, 33], but since the positive fixed point of the growth function is unstable, one cannot expect the profile to approach it.

Based on numerical simulations, Kot conjectured that there is a 'travelling two-cycle', i.e. a pair of wave profiles that alternate between generations and advance at a constant speed [12]. Each of these profiles would connect the zero state with exactly one of the points of the stable two-cycle; please see Figure 9 in [12]. Our own numerical simulations of this scenario give a similar, yet different result, documented in Figure 1. While the solution profile alternately approaches the two values of the stable two-cycle, different parts of the solution propagate at different speeds. There is a first, non-monotone wave front that connects the unstable state $N = 0$ to the unstable state $N = 1$. Then there is a second, monotone front that connects the unstable state $N = 1$ to the stable states of the two-cycle, alternatingly in time. The first front moves faster than the second: the distance between two subsequent "first" fronts is larger that the distance between two subsequent "second" fronts. The purpose of this

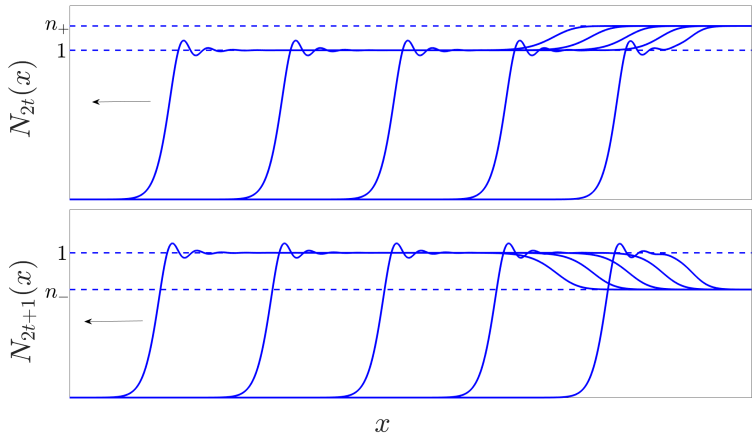

FIG. 1. *Numerical solution of (1), where the logistic growth function F from (4) admits a stable two-cycle and the dispersal kernel K is the Laplace kernel in (16). Solutions are plotted for even (top panel) and odd (bottom panel) generations every 10 time steps. The values n_+ and n_- indicate the high and low density of the two-point cycle for the function F. Parameters are $r = 2.2$ in (4) and $a = 6$ in (16). The initial condition was the characteristic function $N_0(x) = n_+\chi_{[x\geq 10]}$.*

paper is to study this phenomenon of propagation when the map $N \mapsto F(N)$ admits a stable two-cycle.

The subsequent sections are organized as follows. We recall the concept of an 'asymptotic spreading speed' from [30] and review the most important existing results about this speed and related travelling waves. In Section 2, we define a 'generalized spreading speed' and extend the most important results from [30] accordingly. In Section 3, we apply this theory to the second iterate of the operator Q in (1) and show that there exists a generalized spreading speed and corresponding travelling waves. We present numerical simulations of these travelling waves and an explanation of stacked waves in Section 4. We present two directions in which our work can be extended in Section 5. We close with a discussion that identifies several challenging problems in the analysis of integrodifference equations that result from our work.

2. Mathematical Background and Theoretical Set-up. In this section, we give the precise definitions and review the relevant existing results on spreading speeds and travelling waves before we formulate the problem that we will subsequently study.

We shall always assume that the growth function $F \geq 0$ is sufficiently smooth. The precise properties of F will be discussed later. We also assume that the dispersal kernel K is a non-negative, continuous and symmetric function with the property

$$\int K(x)dx = 1. \tag{5}$$

In addition, we assume that the moment-generating function of K, given by

$$M(s) = \int K(x)e^{sx}dx, \tag{6}$$

exists for at least one non-zero value of s.

To define the asymptotic spreading speed, we denote by $C_{[\pi_0,\pi_1]}$ the set of continuous functions on $\mathbb{R}$ with values in the interval $[\pi_0, \pi_1]$, where $0 \leq \pi_0 < \pi_1$. We

can consider any real number as a constant function. In that sense, fixed points of F are spatially constant fixed points of Q. If F is continuous with values between π_0 and π_1, then Q will map $C_{[\pi_0,\pi_1]}$ into itself. For a given initial condition $N_0(x)$ we define the sequence $\{N_t(x)\}$ via the recursion $N_{t+1} = Q[N_t]$ as in (1). The following definition is standard and appears in the literature in slightly different but equivalent formulations [10, 15, 30, 31].

DEFINITION 2.1. *The value c^* is called the* asymptotic spreading speed *of Q if the following conditions hold:*

i) For any $N_0 \in C_{[0,1]}$ with compact support, we have

$$\lim_{t\to\infty} \sup_{|x|\geq ct} N_t(x) = 0 \text{ for all } c > c^*.$$

ii) For any $N_0 \in C_{[0,1]}$ with $N_0 \not\equiv 0$, we have

$$\lim_{t\to\infty} \inf_{|x|\leq ct} N_t(x) = 1 \text{ for all } c \in (0, c^*).$$

The following result is standard and was recently reviewd in [2, 26].

PROPOSITION 2.2. *Let F be a Lipschitz continuous function with values in $[\pi_0, \pi_1]$ and let Q be the operator defined in (1). Then Q is continuous and compact in the topology of uniform convergence on compact subsets in $C_{[\pi_0,\pi_1]}$. More specifically,*

i) (Continuity) If $v_t \to v$ uniformly on compact subsets of $\mathbb{R}$ in $C_{[\pi_0,\pi_1]}$, then $Q[v_t](x) \to Q[v](x)$ for all $x \in \mathbb{R}$.

ii) (Compactness) Every sequence $\{v_t\}$ in $C_{[\pi_0,\pi_1]}$ has a subsequence $\{v_{t_i}\}$ such that $\{Q[v_{t_i}]\}$ converges uniformly on every bounded subset of $\mathbb{R}$.

Under the standing assumptions on the dispersal kernel K, we can formulate conditions on the growth function F that guarantee the existence of a spreading speed. The following is an adaptation of the seminal theorem by Weinberger [30], with additions by Weinberger and Zhao [31].

THEOREM 2.3 (see Theorem 6.5 in [30]). *Assume that the standing assumptions on K hold and let F be a growth function that satisfies the following conditions:*

i) F is bounded and continuously differentiable,

ii) $F(0) = 0$ and $F(1) = 1$ are the only two fixed points of F on $[0, 1]$,

iii) $F'(0) > 1$,

iv) F is non-decreasing on $[0, 1]$.

Then, there exists a spreading speed $c^* > 0$ for the operator Q defined by (1).

Since our operator Q is compact (see Proposition 2.2), the existence of travelling waves is also guaranteed.

THEOREM 2.4 (Theorem 6.6 in [30]). *Let F be a function that satisfies the hypotheses of Theorem 2.3. Then for all $c \geq c^*$, there exists a monotone travelling wave solution $N_t(x) = W(x+ct)$ of (1) with $\lim_{z\to\infty} W(z) = 1$ and $\lim_{z\to-\infty} W(z) = 0$. For $c < c^*$ there exists no such travelling wave solution.*

Moreover, under the additional assumption that the function F is bounded above by its linearization at zero, there is an explicit formula for the spreading speed.

THEOREM 2.5 ([29, 30]). *If, in addition to the assumptions of Theorem 2.3, we have $F(N) \leq F'(0)N$ on $[0, 1]$, then the spreading speed of Q is given by*

$$c^* = \inf_{s\in\Omega} \frac{1}{s} \ln\left(F'(0)M(s)\right), \quad \Omega = \{s > 0 | M(s) < \infty\}. \tag{7}$$

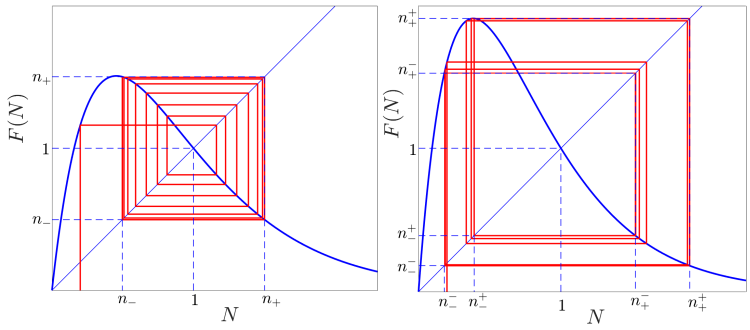

FIG. 2. *A stable two-cycle (left) and four-cycle (right) for the Ricker function with parameter* $r = 2.2$ *(left) and* $r = 2.6$ *(right).*

It is a straightforward calculation to show that the minimal speed of a travelling profile $N_t(x) = W(x + ct)$ for the linear integrodifference equation (1) with $F(N)$ replaced by $F'(0)N$ is also given by the expression for c^* in (7); please see e.g. [13]. If the spreading speed of the nonlinear equation is the same as for the linearized (at zero) equation, then we say that the spreading speed is *linearly determined* [15]. Using the linearization, one obtains a parametric representation of c^* through the pair of conditions [12]

$$c = \frac{M'(s)}{M(s)}, \qquad \text{and} \qquad F'(0) = \frac{e^{sM'(s)/M(s)}}{M(s)}, \tag{8}$$

where M denotes the moment-generating function of K as in (6).

The conditions on the growth function F in Theorem 2.3 are somewhat restrictive. The Beverton-Holt function in (2) satisfies them, independent of the value of R. The Ricker and logistic functions, however, satisfy these conditions only for $0 < r < 1$. When $1 < r < 2$, they both become non-monotone, but $N = 0$ is still an unstable fixed point and $N = 1$ is the globally stable positive fixed point. These two ingredients are sufficient to guarantee that Theorems 2.3, 2.4 and 2.5 hold to the extent possible. One now considers the space $C_{[0,\pi_1]}$, where π_1 is the maximum of the growth function F. One can show that there exists a spreading speed, that it is linearly determined by the formula in (7), and there exist travelling waves, not necessarily monotone, for all speeds greater than or equal to the spreading speed [10, 15, 32, 33]. Numerical simulations of such profiles are shown in Figure 8 in [12] and Figure 2 in [15].

At $r = 2$, the positive state $N = 1$ in the Ricker and logistic functions loses stability through a flip bifurcation, and there is a (globally) stable two-cycle for $2 < r < 2.526$ and $2 < r < 2.449$, respectively [21]. We denote the values of the two-cycle as $n_\pm$. They satisfy the relations $n_+ = F(n_-) = F(F(n_+))$ and $0 < n_- < 1 < n_+$, see Figure 2. Our work is concerned with the behaviour of travelling objects in this case. It is well known that, as r increases further, there is a period doubling bifurcation to a four-cycle (see right plot in Figure 2). We will touch this case in Section 5. Increasing r even further triggers a period-doubling cascade to higher order cycles and chaos.

As mentioned in the introduction, Kot conjectured the existence of a travelling two-cycle for model (1), based on simulations in Figure 9 in [12]. Our simulations in Figure 1 indicate that different parts of the profile travel at different speeds, as explained in the introduction. As is common when studying two-cycles, we introduce

the second-iterate operator $N_{t+2}(x) = \mathcal{S}[N_t](x)$ as

$$\mathcal{S}[N](x) := (Q \circ Q)[N](x) = \int K(x-y)F\left(\int K(y-z)F(N(z))dz\right)dy. \tag{9}$$

When studying the properties of $\mathcal{S}$, it will be convenient to change indices and study $\tilde{N}_{t+1}(x) = \mathcal{S}[\tilde{N}_t](x)$. We will drop the tilde when no confusion can arise. The following properties of $\mathcal{S}$ are a direct consequence of the corresponding properties of Q.

PROPOSITION 2.6. *Under the assumptions of Proposition 2.2, the operator $\mathcal{S}$ is continuous and compact.*

A travelling two-cycle for the operator Q corresponds to a pair of travelling wave profiles for the operator $\mathcal{S}$. Since our simulations in Figure 1 indicate that instead, we expect travelling objects of different speeds for the operator $\mathcal{S}$, we begin by defining an appropriate generalized spreading speed.

DEFINITION 2.7. *The value $c^*_{(\pi_0,\pi_1)}$ is called the generalized asymptotic spreading speed of $\mathcal{S}$ from π_0 to π_1 if the following conditions hold:*

i) For any $N_0 \in C_{[\pi_0,\pi_1]}$ such that $N_0 - \pi_0$ has compact support,

$$\lim_{t\to\infty} \sup_{|x|\geq ct} N_t(x) = \pi_0 \text{ for all } c > c^*_{(\pi_0,\pi_1)}. \tag{10}$$

ii) For any $N_0 \in C_{[\pi_0,\pi_1]}$ such that $N_0 - \pi_0 \not\equiv 0$

$$\lim_{t\to\infty} \inf_{|x|\leq ct} N_t(x) = \pi_1 \text{ for all } c \in (0, c^*_{(\pi_0,\pi_1)}). \tag{11}$$

Please note that for $\pi_0 = 0$, this definition agrees with the standard definition given above, i.e. $c^*_{(0,1)} = c^*$.

We adapt and extend the theory in [30] to establish the existence of a spreading speed and travelling wave solutions for our operator $\mathcal{S}$. We slightly generalize Weinberger's theory by vertically translating functions bounded below by 0 to functions bounded below by $\pi_0 > 0$. The idea behind the proof of the following theorem can be found in the corollary of Proposition 3 in [16].

THEOREM 2.8. *Assume that the operator $\mathcal{U}$ acts on the space $C_{[\pi_0,\pi_1]}$ of continuous functions as follows:*

i) (Translation invariance) $\mathcal{U}[N(\cdot - a)](x) = \mathcal{U}[N](x-a)$.
ii) (Invariance on $C_{[\pi_0,\pi_1]}$) $N \in C_{[\pi_0,\pi_1]} \Rightarrow \mathcal{U}[N] \in C_{[\pi_0,\pi_1]}$.
iii) (Fixed points) $\mathcal{U}[\pi_0] = \pi_0$, $\mathcal{U}[\pi_1] = \pi_1$, $\mathcal{U}[\alpha] > \alpha$ for $\alpha \in (\pi_0, \pi_1)$.
iv) (Monotonicity) $\pi_0 \leq N \leq M \leq \pi_1 \Rightarrow \mathcal{U}[N] \leq \mathcal{U}[M]$.
v) (Continuity) If $\{f_t\} \subset C_{[\pi_0,\pi_1]}$ and $f_t \to f$ uniformly on compact subsets of $\mathbb{R}$ then $\mathcal{U}[f_t] \to \mathcal{U}[f]$ pointwise as $t \to \infty$.

Then there exists a generalized spreading speed $c^*_{(\pi_0,\pi_1)}$ for $\mathcal{U}$ from π_0 to π_1.

Proof. We construct an operator $\widetilde{\mathcal{U}}$ on $C_{[0,\pi_1-\pi_0]}$ as $\widetilde{\mathcal{U}}[f] = \mathcal{U}[f + \pi_0] - \pi_0$. This operator inherits all the qualitative properties from $\widetilde{\mathcal{U}}$, shifted to the interval $[0, \pi_1 - \pi_0$. Hence, it satisfies the assumptions of Theorem 6.5 in [30], which guarantees the existence of a spreading speed. ∎

3. Existence of Spreading Speeds and Travelling Waves. We apply Theorem 2.8 to $\mathcal{U} = \mathcal{S} = Q \circ Q$ and prove the existence of a generalized spreading speed and travelling waves from 1 to n^+. We begin with the case where F is monotone on the interval $[n_-, n_+]$. For the Ricker and logistic functions, the monotonicity condition is satisfied when $2 < r < 2.2565$ and $2 < r < 2.2361$, respectively.

3.1. The Monotone Case.

THEOREM 3.1. *Let F be a growth function that satisfies the following conditions:*

i) F is bounded and continuously differentiable;

ii) F has exactly one stable two-cycle, i.e. there exist $n_\pm$ such that $0 < n_- < 1 < n_+$, and $F(n_-) = n_+$ and $F(n_+) = n_-$, and all non-negative initial conditions converge to this two-cycle under the map $N_{t+1} = F(N_t)$;

iii) $N = 1$ is the only fixed point of F on the interval $[n_-, n_+]$;

iv) $F'(1) < -1$;

v) F is non-increasing on the interval $[n_-, n_+]$.

Then, there exists a spreading speed $c^*_{(1,n_+)}$ for the operator $\mathcal{S}$ in (9) from 1 to n^+.

Proof. Clearly, $\mathcal{S}$ is translation invariant. The function F maps $[1, n_+]$ into $[n_-, 1]$ and vice versa. Hence, if $N \in [1, n_+]$, then $Q[N] \in [n_-, 1]$ and also $Q(Q[N]) \in [1, n_+]$. Therefore, $C_{[1,n_+]}$ is invariant under $\mathcal{S}$. Since $F(1) = 1$ and $F(F(n_+)) = n_+$, we have $\mathcal{S}(1) = 1$ and $\mathcal{S}(n_+) = n_+$ in the sense of constant functions. From *iv)* we have $(F \circ F)'(1) > 1$ and hence $F(F(\alpha)) > \alpha$ for some $\alpha > 1$. Since there is no fixed point between 1 and n_+, we must have $F(F(\alpha)) > \alpha$ for $\alpha \in (1, n_+)$. The same relation holds for constant functions under $\mathcal{S}$. To show monotonicity, assume that $1 \le N(x) \le M(x) \le n_+$. Then by *v)*, we have $1 \ge F(N(x)) \ge F(M(x)) \ge n_-$ and hence also $1 \ge Q[N] \ge Q[M] \ge n_-$. But then we repeat the argument since F maps $[n_-, 1]$ into $[1, n_+]$ and obtain $1 \le Q(Q[N]) \le Q(Q[M]) \le n_+$. Finally, continuity follows from Proposition 2.6. ∎

Along with the existence of a spreading speed, we are able to establish the existence of travelling wave solutions connecting 1 to n_+.

THEOREM 3.2. *Let F be a function that satisfies the hypotheses of Theorem 3.1. Then for all $c \ge c^*_{(1,n_+)}$, there exists a monotone travelling wave solution $W(x + ct)$ with $\lim_{z\to-\infty} W(z) = 1$ and $\lim_{z\to\infty} W(z) = n_+$ for the recursion defined by (9).*

Proof. For $M \in C_{[0,n_+-1]}$ define the operator $M \mapsto \mathcal{S}[M + 1] - 1$. This operator inherits the monotonicity properties from $\mathcal{S}$ and is compact by Proposition 2.6. Hence, the existence of a traveling wave with asymptotic conditions 0 and $n_+ - 1$ follows from Theorem 6.6 in [30]. An upward shift by 1 of this wave gives the desired traveling wave. ∎

Although we have not been able to prove that $c^*_{(1,n_+)}$ is linearly determined, we can linearize $\mathcal{S}$ around $N = 1$ and obtain the slowest speed of a travelling (exponential) profile of the linearized equation. The linearization is given by

$$N_{t+1}(x) = [F'(1)]^2 \int (K * K)(x - y) N_t(y) dy. \tag{12}$$

Analogous to the formula in (7), the spreading speed of this linearized equation is

$$\widehat{c}_{(1,n_+)} = \inf_{s\in\Omega} \frac{1}{s} \ln\left([F'(1)]^2 [M(s)]^2\right), \qquad \Omega = \{s > 0 | M(s) < \infty\}. \tag{13}$$

The term M^2 arises from the properties of the moment-generating function under convolution. In Section 4 we use simulations to discuss how $c^*_{(1,n_+)}$ and $\widehat{c}_{(1,n_+)}$ are related.

3.2. The Non-Monotone Case. An overcompensatory growth function that has a stable two-cycle, given by $\{n_-, n_+\}$, is not necessarily non-increasing in the interval $[n_-, n_+]$. This behaviour arises in the Ricker and logistic functions for $2.2565 <$

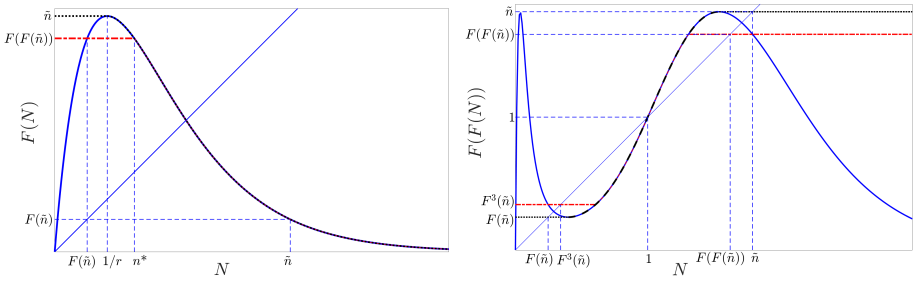

FIG. 3. *Construction of the functions F^+ and F^- in the non-monotone case, where F is the Ricker function with $r = 2.5$. Left panel: Functions F (solid), F^+ (dotted) and F^- (dash-dot). Right panel: Functions $F \circ F$ (solid), $F^+ \circ F^+$ (dotted) and $F^- \circ F^-$ (dash-dot).*

$r < 2.526$ and $2.2361 < r < 2.449$, respectively. Hence, condition v) of Theorem 3.1 is violated in that range. In this case, we can adapt the ideas in [10, 15] to construct sub- and super-solutions that satisfy the conditions of Theorem 3.1 and that bound the iterates of $\mathcal{S}$.

Let F be a function that satisfies the first four hypotheses of Theorem 3.1. Instead of condition *v)*, assume the following (see Figure 3):

v′) There is a point $m \in (n_-, 1)$ such that F is increasing on $[0, m)$ and decreasing on $(m, F(m))$.

Since F is unimodal, there is a unique point $n^* \in (m, 1)$ such that $F(n^*) = F(F(\tilde{n}))$. We define

$$F^+(N) := \begin{cases} \tilde{n}, & 0 \le N \le m, \\ F(N), & N > m, \end{cases} \quad \text{and} \quad F^-(N) := \begin{cases} F(F(\tilde{n})), & 0 \le N \le n^*, \\ F(N), & N > n^*. \end{cases}$$

We use the Ricker function to illustrate this definition. The Ricker function has a unique maximum, and it occurs at $m = 1/r$. The left plot in Figure 3 shows F, F^- and F^+, whereas the right plot shows the respective second iterates. Please note that $F^-(N) \le F(N) \le F^+(N)$ on $[F(\tilde{n}), \tilde{n}]$ and $F^-(N) = F(N) = F^+(N)$ for $N \ge n^*$.

By assumption, the fixed points of $F \circ F$ are precisely n_-, 1 and n_+. Furthermore, we have $(F \circ F)'(1) > 1$. Thus, we find $(F \circ F)(N) < N$ on $(n_-, 1)$. Since $n_- < m < n^* < 1$, we have $F(\tilde{n}) = F(F(m)) < m$ and $F^3(\tilde{n}) = F(F(n^*)) < n^*$. We also obtain $\tilde{n} > m$ and $(F \circ F)(\tilde{n}) > n^*$ since 1 is the only positive fixed point of F, F^+ and F^-. With this information, we can verify that the fixed points of $F^+ \circ F^+$ are $N = F(\tilde{n})$, $N = 1$ and $N = \tilde{n}$, whereas the fixed points of $F^- \circ F^-$ are $N = F^3(\tilde{n})$, $N = 1$ and $N = F(F(\tilde{n}))$, where $F(F(\tilde{n})) \le n_+ \le \tilde{n}$.

We define the second-iterate operators $\mathcal{S}^\pm$ as in (9) with F replaced by $F^\pm$. Then $F^\pm$ satisfy the hypotheses of Theorem 3.1 for $n_+ = \tilde{n}$ and $n_+ = F(F(\tilde{n}))$, respectively.

COROLLARY 3.3. *There exist generalized spreading speeds c^*_+ and c^*_- for the operators $\mathcal{S}^+$ and $\mathcal{S}^-$ from 1 to $\tilde{n}$ and 1 to $F(F(\tilde{n}))$, respectively.*

THEOREM 3.4. *Let F satisfy the conditions of Theorem 3.1 where v) is replaced by v') and define F^+, F^- and $\tilde{n}$ according to the above construction. Assume that the spreading speeds of $\mathcal{S}^\pm$ as above are linearly determined. Then the value of $c^*_{(1,n_+)}$ given by (13) is the spreading speed for $\mathcal{S}$ in the following sense:*

i) For any $N_0 \in C_{[1,\tilde{n}]}$ such that $N_0 - 1$ has compact support,

$$\lim_{t\to\infty} \sup_{|x|\geq ct} N_t(x) = 1 \text{ for all } c > c^*_{(1,n_+)}.$$

ii) For any $N_0 \in C_{[1,\tilde{n}]}$, $N \not\equiv 1$,

$$F(F(\tilde{n})) \leq \lim_{t\to\infty} \inf_{|x|\leq ct} N_t(x) \leq \tilde{n} \text{ for all } c \in (0, c^*_{(1,n_+)}).$$

Proof. By construction of F^+ and F^-, we have the inequalities

$$\mathcal{S}^-[N](x) \leq \mathcal{S}[N](x) \leq \mathcal{S}^+[N](x) \tag{14}$$

for $1 \leq N \leq \tilde{n}$. In fact, for $N \in [1, \tilde{n}]$, we find $\int K(y-z)F(N(z))dz \in [F(\tilde{n}), 1]$. Thus,

$$\begin{aligned} F^-\left(\int K(y-z)F(N(z))dz\right) &\leq F\left(\int K(y-z)F(N(z))dz\right) \\ &\leq F^+\left(\int K(y-z)F(N(z))dz\right). \end{aligned}$$

Given that $F^-(N) = F(N) = F^+(N)$ for $N \geq 1$, we have

$$\begin{aligned} F^-\left(\int K(y-z)F^-(N(z))dz\right) &\leq F\left(\int K(y-z)F(N(z))dz\right) \\ &\leq F^+\left(\int K(y-z)F^+(N(z))dz\right). \end{aligned}$$

Hence, the relations in (14) hold.

By construction, we have $F^-(N) = F(N) = F^+(N)$ near $N = 1$, so that the derivatives of these three functions at $N = 1$ agree. By the assumption that the spreading speeds $c^*_\pm$ of $\mathcal{S}^\pm$ are linearly determined, we have $c^*_+ = c^*_- = c^*_{(1,n_+)}$ from the formula in (13). We now proceed to proving i) and ii) from the statement.

i) Let $N_0 \in C_{[1,\tilde{n}]}$ such that $N_0 - 1$ has compact support. If $N_t = \mathcal{S}^t(N_0)$ and $N^+_t = (\mathcal{S}^+)^t(N_0)$, then by the comparison principle (Proposition 4.1 in [30])

$$1 \leq N_t(x) \leq N^+_t(x).$$

Applying (10) with $\pi_0 = 1$ to the previous inequality gives us our result.

ii) Let $N_0 \in C_{[1,\tilde{n}]}$, $N \not\equiv 1$ and $M_0 = \min\{N_0, F(F(\tilde{n}))\}$. Then $M_0 \leq N_0$ and $M_0 \in C_{[1,F(F(\tilde{n}))]}$, $M_0 \not\equiv 1$. Since F^- is non-increasing, $(\mathcal{S}^-)^t(M_0) \leq (\mathcal{S}^-)^t(N_0)$. If $M^-_t = (\mathcal{S}^-)^t(M_0)$, $N_t = \mathcal{S}^t(N_0)$ and $N^+_t = (\mathcal{S}^+)^t(N_0)$, then by the comparison principle

$$1 \leq M^-_t \leq N_t \leq N^+_t.$$

We get our result by applying (10) with $\pi_1 = F(F(\tilde{n}))$ to the sequence $\{M^-_t\}$ and $\pi_1 = \tilde{n}$ to the sequence $\{N^+_t\}$. ∎

The previous theorem does not guarantee that the solution $N_t(x)$ converges to n^+ but only gives an interval for $N_t(x)$. In the corresponding case for the operator Q with a non-monotone growth function F that has an unstable fixed point at 0 and a

stable fixed point at 1, the authors in [10] were able to guarantee the corresponding limit of 1. Unfortunately, we cannot directly apply their result to our operator $\mathcal{S}$. However, we expect the solution to have a limit at n_+ when the 2-cycle is stable. This expectation is based on the numerical evidence that we discuss in the next section. A more generalized approach, like the one in [32], would be needed to prove this statement. When the two-cycle for the non-spatial map is unstable, we cannot expect convergence to n_+. Instead, the non-spatial map will have cycles of longer period. We discuss these in Section 5.1.

The results regarding the existence of a spreading speed and travelling wave solutions for operator $\mathcal{S}$ from 1 to n_+ stated in this section also apply to $\mathcal{S}$ from 1 to n_-, by application of operator Q to the solution $N_t(x)$.

4. Numerical Results and Interpretation. In this section, we illustrate our theoretical results from the previous section with numerical simulations. We compare the numerically obtained spread rates with the formula in (13) for $\widehat{c}_{(1,n_+)}$ that results from the linearization at the unstable steady state. We show that there is a good agreement between the two quantities. We also define a different 'second-iterate operator' and compare the behaviour of solutions of the two.

For all examples and numerical simulations, we employ the two most frequently used dispersal kernels (together with their moment-generating functions), which are the Gaussian kernel

$$K(x) = \frac{1}{\sqrt{2\pi\sigma^2}} e^{-\frac{x^2}{2\sigma^2}} \qquad \text{with} \qquad M(s) = e^{\frac{\sigma^2 s^2}{2}}, \tag{15}$$

and the Laplace kernel

$$K(x) = \frac{a}{2} e^{-a|x|} \qquad \text{with} \qquad M(s) = \frac{a^2}{s^2 - a^2}. \tag{16}$$

Setting $a = \sqrt{\frac{2}{\sigma^2}}$ guarantees that both kernels have the same variance.

4.1. An Alternative 'Second-iterate' Operator. The second-iterate operator $\mathcal{S} = Q \circ Q$ that we study describes two growth and two dispersal phases, alternating over two generations. Ultimately, we are interested in the spreading speed of this operator, which is an asymptotic quantity that arises in the limit when the number of growth and dispersal phases approaches infinity. One can then ask whether and how much the order of events in the short term matters for this quantity in the long term.

To explore this question, we formulate the operator

$$\tilde{\mathcal{S}}[N](x) = \int (K * K)(x - y)(F \circ F)(N(y)) dy, \tag{17}$$

that describes two growth phases followed by two dispersal phases. The operators $\mathcal{S}$ and $\tilde{\mathcal{S}}$ describe slightly different order of events, but the same number of each of the events. Operator $\tilde{\mathcal{S}}$ is much easier to study since it has the same form as operator Q and fits the framework by Weinberger [30] and others.

In the following, we will first show that the two operators have the same spreading speed from 0 to 1 in the monostable case. Then we will show why the spreading speed of $\tilde{\mathcal{S}}$ from 1 to n^+ is easier to study than that of $\mathcal{S}$. This discussion will also clarify that the operators have the same spreading speed if that speed is linearly determined. In Section 5.2, we will give an example that shows that no such result can hold for the bistable case.

4.2. The Spreading Speed. We begin with the well-known case when the growth function is monotone and concave down, i.e. it satisfies the hypotheses of Theorem 2.5. Then the operator Q has an asymptotic spreading speed from 0 to 1 that we denote by c^*. It is given explicitly by the formula in (7). It follows that the operator $\mathcal{S}$ also has a spreading speed from 0 to 1 and that its value is given by $2c^*$.

Since the growth function F satisfies the hypotheses of Theorem 2.5, so does its second iterate $F \circ F$. Thus, from the theory in [30] we conclude that a spreading speed $\tilde{c}^*$ exists for the operator $\tilde{\mathcal{S}}$ from 0 to 1 and that it is given by the expression:

$$\tilde{c}^* = \inf_{s \in \Omega} \frac{1}{s} \ln \left((F \circ F)'(0) \int e^{sx} (K * K)(x) dx \right),$$

where Ω denotes the values of $s > 0$ for which the moment-generating function of K exists. Since $F'(F(0)) = F'(0)$ and since the moment-generating function of a convolution is the product of moment-generating functions, we conclude that operators $\mathcal{S}$ and $\tilde{\mathcal{S}}$ have the same spreading speed from 0 to 1.

We can use the parametrization provided by equations (8) to calculate an explicit formula for c^* [12]. In the case of the Gaussian kernel (15), we obtain

$$c^* = \sqrt{2\sigma^2 \ln(F'(0))}. \tag{18}$$

In the case of the Laplace kernel (16), the parametric equations in (8) result in

$$c = \frac{2s}{a^2 - s^2}, \qquad F'(0) = \frac{a^2 - s^2}{a^2} \exp\left(\frac{2s^2}{a^2 - s^2} \right) = \frac{2}{e^2} \frac{a^2 - s^2}{2a^2} \exp\left(\frac{2a^2}{a^2 - s^2} \right).$$

The latter equation is of the form $\rho z = e^z$ and can be solved by the Lambert W function (see e.g. [4])

$$\frac{2a^2}{a^2 - s^2} = -W\left(-\frac{2}{F'(0)e^2} \right).$$

For real values s, we need to choose the branch W_{-1} of the Lambert W function [2] and obtain

$$s = a \sqrt{\frac{2}{W_{-1}\left(-\frac{2}{F'(0)e^2} \right)} + 1}. \tag{19}$$

Substituting (19) into (8), we obtain an explicit expression for the speed as

$$c^* = -\frac{1}{a} W_{-1}\left(-\frac{2}{F'(0)e^2} \right) \sqrt{\frac{2}{W_{-1}\left(-\frac{2}{F'(0)e^2} \right)} + 1}. \tag{20}$$

This expression is novel. It still requires computation for the Lambert W function, but since many modern software packages have this function built in, our formula becomes easier to use than the root-finding algorithm previously proposed in [12].

All the results so far hold when the growth function is monotone on $[0, 1]$. In addition, the spreading speed of Q is still linearly determined when the growth function is not monotone but has $N = 1$ as a stable fixed point. If we drop the requirement that the density behind the front converges to the steady state and instead require only that it be bounded below by a positive number, then there is still a 'spreading speed'

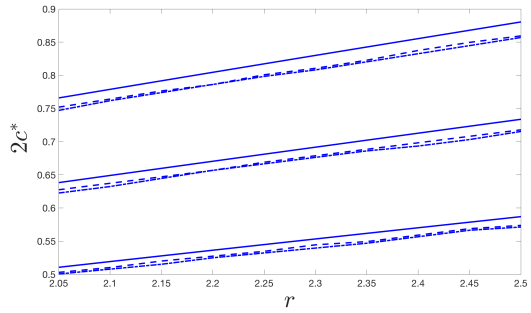

FIG. 4. *Theoretical (solid line) and numerical spreading speeds for operators $\mathcal{S}$ (dashed line) and $\tilde{\mathcal{S}}$ (dash-dot line) from 0 to 1 with Ricker function and Laplace kernel for different values of a (top: $a = 10$, middle: $a = 12$, bottom: $a = 15$) with respect to parameter r. The plot is generated with a scheme that uses the FFT algorithm and is based on [23].*

and it is linearly determined [10, 15, 32, 33]. Hence, the explicit expressions (19, 20) give the spreading speed for the Ricker and logistic functions even when $r > 1$.

We compare the numerical spreading speeds obtained from simulations to the values predicted by formulas (18) and (20). We illustrate the plot obtained for the Laplace kernel and the Ricker function in Figure 4, with respect to the parameter r of the growth function. Similar plots are obtained when K is the Gaussian kernel and when F is the logistic function. In all cases, the numerical errors are bounded above by 5%. An error of this magnitude is standard for spread problems [23].

4.3. The Generalized Spreading Speed from 1 to n_+. When the growth function F satisfies the hypotheses of Theorem 3.1, operators $\mathcal{S}$ and $\tilde{\mathcal{S}}$ have generalized spreading speeds $c^*_{(1,n_+)}, \tilde{c}^*_{(1,n_+)}$ from 1 to n_+. The linearizations of $\mathcal{S}$ and $\tilde{\mathcal{S}}$ at $N = 1$ are identical. Sufficient conditions for linear determinacy of $\tilde{c}^*_{(1,n_+)}$ for $\tilde{\mathcal{S}}$ follow directly from [30], but not for $\mathcal{S}$. Somewhat surprisingly, these sufficient conditions for $\tilde{\mathcal{S}}$ are met when F is the logistic growth function, but not for the Ricker function, as we show below. Nonetheless, our simulations indicate that the generalized spreading speed for $\tilde{\mathcal{S}}$ is linearly determined in both cases and that the speeds for $\tilde{\mathcal{S}}$ and $\mathcal{S}$ are identical.

PROPOSITION 4.1. *Let F be the logistic function. Then the generalized spreading speed of $\tilde{\mathcal{S}}$ from 1 to n_+ is linearly determined.*

Proof. We begin by showing that $(F \circ F)''(N) \leq 0$ on $[1, n_+]$. Indeed,

$$(F \circ F)''(N) = -2r(1+r)(2+r) + 12[r^2(1+r)N - r^3N^2]. \tag{21}$$

The roots of (21) are given by the expression

$$N = \frac{3(1+r) \pm \sqrt{3(r^2-1)}}{6r}.$$

By solving the inequality

$$\frac{3(1+r) + \sqrt{3(r^2-1)}}{6r} - 1 < 0,$$

we conclude that both roots of (21) are less than 1 when $r > 2$. It follows that

$(F \circ F)''(N) \leq 0$ for all $N \geq 1$. By the mean value theorem,

$$(F \circ F)(N) \leq [F'(1)]^2(N-1) + 1$$

on $[1, n_+]$. Thus, the spreading speed of $\tilde{\mathcal{S}}$ is linearly determined (similarly to the result of Theorem 2.5). ∎

We now find explicit expressions for the generalized spreading speed of $\tilde{\mathcal{S}}$ from 1 to n_+ with the logistic growth function and the two dispersal kernels. Since the speed is linearly determined, we can use the formula in (13) or the corresponding (adapted) parametrization from (8). Since the moment-generating function of $K * K$ is simply the square of the moment-generating function of K, we find the expressions:

$$c = \frac{2M'(s)}{M(s)} \qquad \text{and} \qquad [F'(1)]^2 = \frac{e^{2sM'(s)/M(s)}}{M(s)^2}. \tag{22}$$

When K is the Gaussian kernel, we easily find the speed as

$$c^*_{(1,n_+)} = 2\sqrt{\sigma^2 \ln[F'(1)]^2}. \tag{23}$$

When K is the Laplace kernel, we can derive an expression in terms of the Lambert W function in a similar manner as (20) (for details, see [2]), namely

$$c^*_{(1,n_+)} = -\frac{2}{a} W_{-1}\left(-\frac{2}{|F'(1)|e^2}\right) \sqrt{\frac{2}{W_{-1}\left(-\frac{2}{|F'(1)|e^2}\right)} + 1}. \tag{24}$$

We compare the values given by (24) to simulations (Figure 5, left plot); the results for the Gaussian kernel are similar. All three curves match very well, indicating that the generalized spreading speed for $\mathcal{S}$ could be linearly determined. The discrepancy between theoretical and numerical results are again within 5%.

Finally, we turn to the Ricker function from (3). The second derivative of $F \circ F$ can easily be evaluated as $(F \circ F)''(1) = r(r-1)(r-2)^2$. The following lemma highlights the difference between the Ricker and the logistic function.

LEMMA 4.2. *Let F be the Ricker function with $r > 1$. Then $(F \circ F)''(1) > 0$, i.e. F is concave up near $N = 1$. In particular, exists some $\alpha > 1$ such that $(F \circ F)(N) \geq [F'(1)]^2(N-1) + 1$ on $[1, \alpha]$.*

According to the lemma, the function $F \circ F$ is not bounded by its linearization near $N = 1$. We also have $(F \circ F)'(1) > 1$. It follows that the function $F \circ F$ exhibits what is called a 'weak Allee effect' at $N = 1$ [27], and does not satisfy the sufficient condition for linear determinacy from [30].

For reaction-diffusion systems, it was shown that if the Allee effect is sufficiently weak, then the spreading speed is linearly determined [27]. Although some analysis has been done regarding Allee effects in integrodifference equations [28], it is unclear how to characterize an Allee effect as sufficiently weak. Our numerical simulations suggest that formulas (23) and (24) still represent the generalized spreading speed for operator $\tilde{\mathcal{S}}$, with this weak Allee effect (see Figure 5, right plot).

Since the operators $\mathcal{S}$ and $\tilde{\mathcal{S}}$ have the same linearization at $N = 1$, and since the numerical simulations show such a good agreement between the respective speeds, we formulate the following conjecture.

CONJECTURE. *Let $\mathcal{S}$ be the operator defined by expression (9). Assume F is the Ricker function or the logistic function with $r > 2$. Then the generalized spreading speed $c^*_{(1,n_+)}$ of $\mathcal{S}$ from 1 to n_+ is linearly determined, and is thus given by (13).*

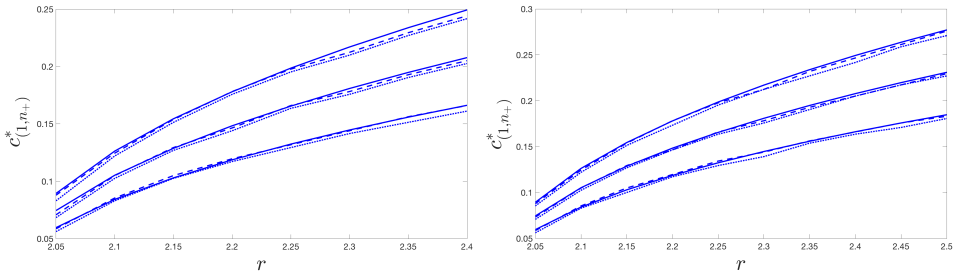

FIG. 5. *Theoretical (full line) and numerical generalized spread speeds of operators $\mathcal{S}$ (dashed line) and $\tilde{\mathcal{S}}$ (dash-dot line) from 1 to n_+, with Laplace dispersal kernel and logistic growth function (left) or the Ricker growth function (right). The speeds are plotted for different values of a (top: $a = 10$, middle: $a = 12$, bottom: $a = 15$) with respect to parameter r. The plot is generated with a scheme that uses the FFT algorithm and is based on [23].*

4.4. Stacked Fronts. We can now explain the behaviour of solutions that we observed in Figure 1. The operator $\mathcal{S}$ has two spreading speeds. One is simply twice the spreading speed of Q and is defined by the linearization at 0. When $r > 2$ so that the positive steady state of Q is unstable, the exact behaviour behind the front is unclear. The other generalized spreading speed exists only when the positive state of Q is unstable and a stable two-cycle exists. We conjecture that this second speed is given by the linearization at 1. We proved the existence of travelling waves connecting the states 1 and n_+ (n_-) for the operator $\mathcal{S}$ under certain conditions.

The simulations in Figure 1 show what has been termed 'stacked fronts' [20]: There is a non-monotone travelling front between the unstable states 0 and 1. This front travels at the speed determined by the linearization at 0. In behind, the travelling wave that connects 1 to n_+ (or n_-) forms a second, stacked, front that propagates at the speed given by the linearization at 1. The two cases for $\mathcal{S}$ (i.e. the connection of the second front to n_+ or n_-) appear as alternating profiles in the operator Q. Only in that sense, but not in the strict sense, we have a 'travelling two-cycle' [12].

We can observe a stacked front only if the profile that starts at 0 moves faster than the profile starting at 1. If that is the case, we see a plateau emerging at $N = 1$. The length of the plateau at $N = 1$ increases with time, giving the impression of stability, even though this state is unstable for the map $N \mapsto F(N)$ when $r > 2$. This type of behaviour for solutions was first observed in the context of a system of reaction-diffusion equations in [18], and was termed as *dynamical stabilization*.

From the two explicit formulas for the spreading speeds, we calculate whether the first profile actually travels faster, i.e. whether we have $2c^* > c^*_{(1,n_+)}$. For the speeds reported in Figures 4 and 5 (right plot), this relationship certainly holds. In general, in the case of the Gaussian kernel, we use equations (18) and (23) to obtain

$$\frac{2c^*}{c^*_{(1,n_+)}} = \sqrt{\frac{\ln(F'(0))}{\ln(|F'(1)|)}}.$$

When F is the Ricker function or the logistic function, we have $F'(0) > |F'(1)|$ for $r > 2$ so that $2c^* > c^*_{(1,n_+)}$. The same conclusion holds for the Laplace kernel, but the derivation is a bit more involved, see [2]. In both cases, the result is independent of the variance of the kernel.

The condition that the first profile travel faster than the second is necessary but not sufficient for the emergence of a plateau [19]. Figure 6 shows that the oscillatory

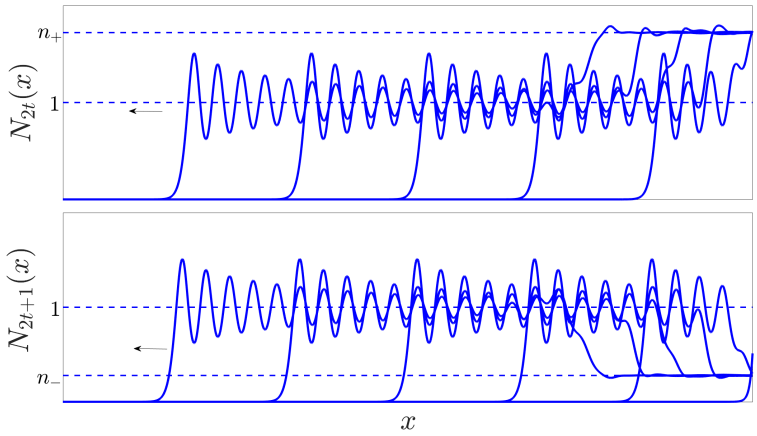

FIG. 6. *Numerical solution of the integrodifference equation, where F is the Ricker function with $r = 2.525$, and K is the Laplace kernel with $a = 15$, plotted for even (top panel) and odd (bottom panel) generations every 10 time steps. The values n_+ and n_- are the high and low density point cycle. $N_0 = n_+\chi_{[x\geq 10]}$.*

decay to the dynamically stabilized positive state can be so slow that no plateau emerges for at least 50 generations. We also do not see the connection to n^+ emerge as a constant profile with constant speed.

5. Extensions. Our results on how two-cycles in the growth function can translate into generalized spreading speeds and travelling waves for the second-iterate operator are the basis for several possible extensions. We list two of them in this section.

5.1. Four-cycles. As r increases, the two-cycle of the Ricker or logistic function undergoes a period-doubling bifurcation and gives rise to a stable four-cycle, that we denote by n_-^-, n_-^+, n_+^- and n_+^+, (Figure 2, right plot). In [12], the author plotted a 'travelling four-cycle' in this case. Our simulations reveal that, again, the profile consists of several parts that move at different speeds. As in Figure 1, we observe a leading profile from 0 to 1 that moves the fastest, followed by a second, slower profile that connects 1 to n_+ or n_-. Eventually, there emerges an even slower third profile that connects n_+ to n_+^+ in the top left panel, and correspondingly other points on the four-cycle in the other panels. In each panel of Figure 7, we plot the solutions of $N_{t+1} = Q[N_t]$ every 10 generations. Each panel corresponds to a different generation modulo 4. To focus on the second and third profiles, we do not show the leading profile in these plots. We notice the emergence of a plateau at all unstable fixed points of F, i.e. at $1, n_+, n_-$. We can extend the ideas and theory developed above and study the fourth-iterate map of Q or the second-iterate map of $\mathcal{S}$.

Since operator $\mathcal{S}$ satisfies the continuity and compactness properties required for the existence of a spreading speed and travelling waves, the operator $\mathcal{S} \circ \mathcal{S}$ does also. The following theorem is analogous to Theorems 3.1 and 3.2.

THEOREM 5.1. *Let F be a growth function with the following properties:*

i) F is bounded and Lipschitz continuous;

ii) F has exactly one stable four-cycle (n_+^+, n_-^-, n_+^-, n_-^+), which corresponds to two stable two-cycles in $F \circ F$, given by (n_-^-,n_-^+) and (n_+^-, n_+^+);

iii) $N = n_+$ is the only fixed point of $F \circ F$ on the interval $[n_+^-, n_+^+]$;

iv) $(F \circ F)'(n_+) < -1$;

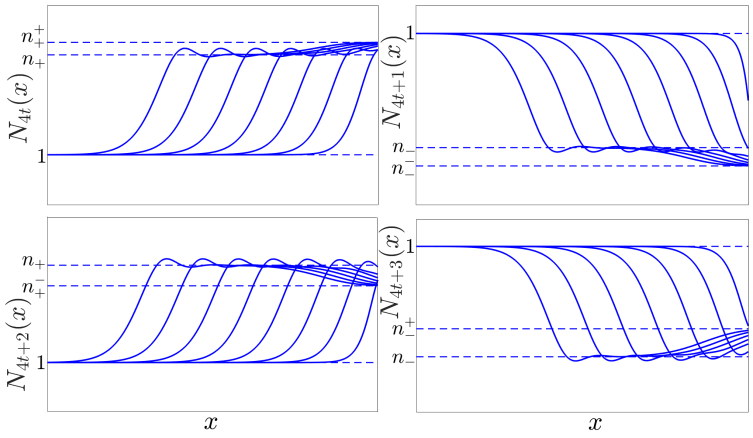

FIG. 7. *Four travelling profiles emerge when the growth function has a stable four-cycle. Numerical solution of the integrodifference equation in (1), with logistic growth function and Laplace dispersal kernel. Solutions are plotted every* 10 *generations with remainders 0 (top left), 1 (top right), 2 (bottom left) and 3 (bottom right) modulo 4. Th values* n_+ *and* n_- *indicate the high and low density of the two-point cycle for the function F. Values* n_+^+, n_+^-, n_-^+ *and* n_-^- *form the four-cycle. Parameters are* $r = 2.5$ *in (4) and* $a = 6$ *in (16). The initial condition was the characteristic function* $N_0(x) = \chi_{[x<10]} + n_+^+ \chi_{[x\geq 10]}$.

v) F is non-increasing on $[n_+^-, n_+^+]$ *and non-decreasing on* $[n_-^-, n_-^+]$.
Then, there exists a generalized spreading speed $c^*_{(n_+, n_+^+)}$ *for the operator* $\mathcal{S}\circ\mathcal{S}$ *from* n_+ *to* n_+^+. *Furthermore, for all* $c \geq c^*_{(n_+, n_+^+)}$, *there exists a monotone travelling wave solution* $W(x+ct)$ *with* $\lim_{z\to-\infty} W(z) = n_+$ *and* $\lim_{z\to\infty} W(z) = n_+^+$ *for the recursion defined by* $\widehat{N}_{t+1} = (\mathcal{S}\circ\mathcal{S})[\widehat{N}_t]$.

5.2. Bistable Wave. With the emergence of a stable two-cycle for the growth function F, there are two stable fixed points of $F \circ F$, namely n_+ and n_- and an unstable fixed point at 1 in between. These three fixed points translate into corresponding spatially constant fixed points of the operators $\mathcal{S}$ and $\tilde{\mathcal{S}}$. This situation is reminiscent of the so-called 'bistable' scenario of the operator Q that arises when the growth function F has 0 and 1 as stable fixed points and some intermediate unstable fixed point. Ecologically, this situation corresponds to a 'strong Allee effect' where a minimum population density is required for population growth.

The authors in [16, 28] studied the existence of monotone travelling waves connecting two stable fixed points in equation (1). The situation is markedly different from the 'monostable' case that we reviewed in Theorems 2.3 and 2.4. In the bistable case, one can show that there exists a travelling wave profile for exactly one speed, c_b, and this speed can have either sign, i.e. the population density may advance or retreat. The sign of the speed is given by the sign of the integral $\int_0^1 [F(n) - n]dn$ [28].

It turns out that our approach of upward shift from the previous section applies directly to the operator $\tilde{\mathcal{S}}$ but not to $\mathcal{S}$. Symmetry, however, gives important insights into the dynamics for $\mathcal{S}$, which we verify through numerical simulations below.

THEOREM 5.2. *Let the assumptions of Theorem 3.1 be satisfied. Then for the operator* $\tilde{\mathcal{S}}$ *there exists a unique speed* c_b *and a monotone travelling wave profile* W *with* $\lim_{z\to-\infty} W(z) = n_-$ *and* $\lim_{z\to\infty} = n_+$ *so that* $W(\cdot - c_b) = \tilde{\mathcal{S}}[W]$. *Furthermore,*

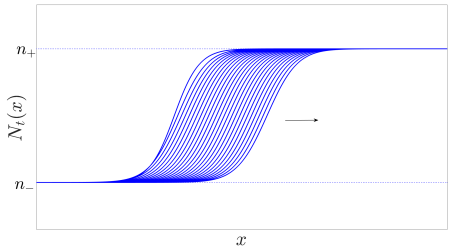

FIG. 8. *Bistable wave for $\widetilde{\mathcal{S}}$. Numerical solution of the integrodifference equation in (1), with logistic growth function and Laplace dispersal kernel. Solutions are plotted every other generation. Parameters are $r = 2.2$ and $a = 15$. The initial condition is the step function $N_0 = n_-\chi_{[x<0]} + n_+\chi_{[x\geq 0]}$*

the sign of c_b is given by the sign of

$$\int_{n_-}^{n_+} [(F \circ F)(n) - n]dn. \tag{25}$$

The proof of this theorem follows from applying the same construction as in Theorem 2.8 for the operator $\tilde{\mathcal{S}}$ to the results in [16, 28].

When $2 < r < 2.2564$ and $2 < r < 2.2361$ for the Ricker function and logistic function, respectively, then the conditions of the theorem (in particular monotonicity) are satisfied. For the logistic function, the values of $n_\pm$ are explicitly given by the expressions

$$n_\pm = \frac{1}{2r}\left[r + 2 \pm \sqrt{r^2 - 4}\right].$$

The integral in (25) can be calculated as

$$\int_{n_-}^{n_+} [(F \circ F)(n) - n]dn = G(n_+) - G(n_-),$$

where

$$G(n) = \frac{2r + 2^2}{2}n^2 - \frac{r(1+r)(2+r)}{3}n^3 + \frac{r^2(1+r)}{2}n^4 - \frac{r^3}{5}n^5.$$

Evaluating this expression numerically, it turns out that the integral is negative whenever the two-cycle is stable (i.e. $2 < r < 2.449$). In particular, the bistable wave is always retreating. We illustrate the resulting front in Figure 8.

Studying the existence of a bistable wave for operator $\mathcal{S}$ turns out to be more difficult. We cannot directly apply the results of [16, 28], as they require an operator of the form in (1). A more generalized theory of bistable travelling waves in monotone semiflows is provided in [6]. However, applying the results by those authors to our case would require the relation $c^*_{(1,n_+)} - c^*_{(1,n_-)} > 0$. Since, by symmetry, we have $c^*_{(1,n_+)} = c^*_{(1,n_-)}$, we cannot use their methods. Similarly, neither of the techniques in [16] or [6] carry over to prove uniqueness of the speed for a travelling wave. But, assuming uniqueness, we can prove that the speed has to equal zero.

PROPOSITION 5.3. *Let the assumptions of Theorem 3.1 be satisfied. Assume furthermore that there is a unique speed c_b for which the operator $\mathcal{S}$ admits a travelling wave with $\lim_{z\to-\infty} W(z) = n_-$ and $\lim_{z\to\infty} W(z) = n_+$. Then $c_b = 0$.*

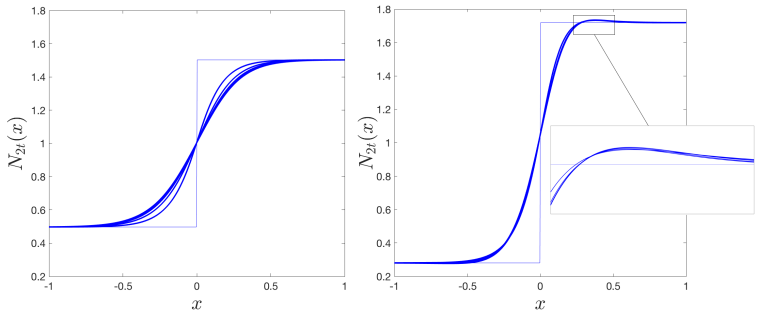

FIG. 9. *Bistable standing wave for $\mathcal{S}$. Numerical solution of the integrodifference equation in (1), with Ricker growth function and Laplace dispersal kernel. Solutions are plotted every other generation. Parameters are $r = 2.2$ (left plot), $r = 2.52$ (right plot) and $a = 10$. The initial condition is the step function $N_0 = n_- \chi_{[x<0]} + n_+ \chi_{[x\geq 0]}$*

Proof. Let c_b be the speed and W the profile of the corresponding wave with asymptotic behaviour as in the statement. Then $\widehat{W}(z) = -W(z)$ is a travelling wave of $\mathcal{S}$ with speed $-c_b$ and asymptotic behaviour $\lim_{z\to-\infty} \widehat{W}(z) = n_+$ and $\lim_{z\to\infty} \widehat{W}(z) = n_-$. Applying the operator Q to W, we obtain a travelling wave $\widetilde{W}(z) = Q[W](z)$ with speed c_b and asymptotic behaviour $\lim_{z\to-\infty} \widetilde{W}(z) = n_+$ and $\lim_{z\to\infty} \widetilde{W}(z) = n_-$ of the operator $\mathcal{S}$. Hence, we have a wave with speed c_b and one with speed $-c_b$ and identical asymptotic behaviour. By the uniqueness of the speed, we require $c_b = 0$. ∎

Numerical simulations illustrate the prediction of the proposition: the wave comes to a halt after a few iterations; see Figure 9. The argument in Proposition 5.3 does not require monotonicity of the wave profile. The left panel in Figure 9 corresponds to the case that the growth function F is monotone in the interval $[n_-, n_+]$, and we see a monotone profile emerge. The panel on the right is for the case when F is not monotone. Correspondingly, we see a non-monotone profile establish.

6. Discussion. Integrodifference equations are discrete-time, continuous-space models to understand biological invasions [13]. Like reaction-diffusion equations, their continuous-time counterparts, integrodifference equations can support travelling waves. Scalar differential equations have monotone dynamics, and accordingly, scalar reaction-diffusion equations have monotone travelling waves. Scalar difference equations can have non-monotone dynamics and, accordingly, integrodifference equations may have non-monotone waves [1]. This difference is crucial in applications since, for example, many insect species exhibit non-monotone (overcompensatory) dynamics [3]. The theory of spreading speeds and travelling waves is well developed in the monotone case. We clarify previous conjectures [12] and contribute to our understanding of non-monotone phenomena [10, 15, 33].

Our main results are that integrodifference equations with overcompensation can support several spreading speeds and associated travelling waves that connect various fixed points and periodic orbits of the underlying growth function, and that these should be studied by analyzing appropriate iterates of the operator Q. Our numerical results show that the different spreading speeds manifest themselves in the form of stacked waves of these iterates. Previous authors proved the existence of travelling waves with overcompensation [10, 15]. Based on our results, we conjecture that these travelling waves are unstable for the integrodifference equation. Instead, the theory

of stacked waves should be developed further. This theory is partially developed for reaction-diffusion equations where vector-valued models are required to study the phenomenon [7, 11, 24]. Integrodifference equations offer an opportunity for deeper understanding using scalar equations. Stacked waves in vector-valued integrodifference equations were recently found in a disease model [20].

The different speeds of the different wave fronts lead to 'dynamical stabilization' [18, 19, 25], i.e. the appearance of a plateau of increasing length that separates the initial 'invasion' from the final state of a two-cycle. In an ecological context, this observation means that a population that had spread into a certain region long ago and had been stable for a long time could suddenly exhibit periodic fluctuations. While the typical question would then be whether any changes in biotic or abiotic conditions caused the instability, our results show a different possibility: the steady state may have been unstable all along, stabilized temporarily by dispersal and spread.

We showed that our approach can be extended to study travelling waves and generalized spreading speeds in cases where the growth function has a four-cycle. As parameter r increases, the Ricker and logistic equations are known to have a sequence of period-doubling bifurcations that can generate cycles of length 2^k (among others). Our techniques and theory generalize to these longer cycles as well. However, the existence of a generalized spreading speed and/or a corresponding travelling wave does not necessarily imply that these objects are stable and that we see them in simulations [2]. Heuristically, as r increases, the quantity $|F'(1)|$ increases and the state $N = 1$ becomes harder to stabilize. Dynamic stabilization does not occur any more and solutions exhibit oscillatory-like behaviour [2].

In addition to the ecologically correct second iterate $\mathcal{S}$, we introduced the operator $\tilde{\mathcal{S}}$ that corresponds to two growth phases followed by two dispersal phases. It is not a second-iterate operator but describes the same number of events as $\mathcal{S}$, only in a different order. The advantage of $\tilde{\mathcal{S}}$ is that its particular form allows one to directly apply the results by previous authors (e.g. [30]) to prove the existence and, in cases, linear determinacy of spreading speeds and of travelling waves. Interestingly, we found that the results for the Ricker and logistic growth function differ in that only with the latter does the linearization of $\tilde{\mathcal{S}}$ at 1 satisfy the subtangential condition for linear determinacy. Numerically, we found that the spreading speeds of $\mathcal{S}$ and $\tilde{\mathcal{S}}$ matched in the case of monostable waves. Future research will prove or disprove this result in general. Interestingly, the two operators make very different predictions in the case of bistable waves. More research is needed to understand the behaviour of bistable waves for $\mathcal{S}$.

So far, results were based on the assumption of a symmetric dispersal kernel. Asymmetry complicates the analysis since we have to consider one spreading speeds in each direction. Several authors studied aspects of asymmetry for the operator Q, even for non-monotone dynamics [32] and stacked waves [20]. A particular form of asymmetry arises from biased dispersal, for example due to stream flow, ocean currents or prevailing wind direction [8, 17, 20]. With biased dispersal, the spreading speed can be positive in the direction of the bias but negative in the opposite direction, even with a monotone and monostable growth function. In river ecosystems, a negative spread rate in the upstream direction has been interpreted as a downstream washout of the species [17]. A very simple form of asymmetry arises from a shift in the dispersal kernel, for example a Gaussian kernel with non-zero mean. While this kernel is still symmetric around its mean, very simple models of biased movement can also generate kernels that are not symmetric around their mean [17]. We present an initial numerical simulation of our model with overcompensation and an asymmetric

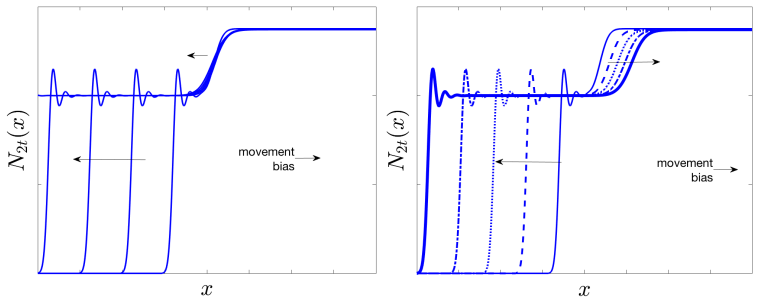

FIG. 10. *Plateau evolving for asymmetric dispersal. Numerical solution of the integrodifference equation in (1), with Ricker growth function and Gaussian dispersal kernel* $K(x) = \mathcal{N}(x; \mu, \sigma^2)$, *where* $\mathcal{N}$ *is the normal distribution with mean* μ *and variance* σ^2. *Solutions are plotted every* 10 *generations. Parameters are* $r = 2.1$ *in (3),* $\sigma^2 = 0.1$, $\mu = 0.1$ *(left plot) and* $\mu = 0.2$ *(right plot). The initial condition was the characteristic function* $N_0(x) = 1.5\chi_{[x\geq 0]}$. *The Gaussian distribution was chosen because there is a standard way to include asymmetry as a non-zero mean, whereas several options exist for the Laplace kernel [17]. The variance was chosen to match the variance of a (symmetric) Laplace kernel with* $a = 15$ *as in some previous Figures.*

(shifted) Gaussian dispersal kernel. We find that the spreading speeds of the first and second wave front may have opposite signs (Figure 10). In this case, the plateau that emerges through dynamic stabilization expands in both directions.

We finish our discussion with another analytical challenge. Li and co-authors proved the existence of a travelling wave in the case that the growth function has a stable two-cycle [15]. They illustrated the shape of such profiles by fixed-point iteration, i.e. by numerically solving the equation $N = Q[N(\cdot - c^*)]$, after calculating c^* from the linearized formula. For certain parameter values, they found a profile that connects the zero state to a spatially periodic pattern that alternates between n_- and n_+, see Figure 3 in [15]. They conjectured that the period of the pattern behind the wave equals twice the speed of the wave. They used a dispersal kernel with a variance much smaller than all simulations presented in our previous figures.

Despite intensive numerical simulations (for very small variance), we did not observe such a profile emerge for the dynamic equation in that parameter range from a piecewise constant initial condition that we had used in all the Figures so far. With a (scaled) normal distribution as initial condition, we observed phenomena on two time scales. On a fast scale, within only a few iterations, we observed a moving profile that connects zero to a spatially oscillating pattern; see Figure 11. This profile is vaguely reminiscent of the profile in Figure 3 in [15], but it moves faster than the linearization at zero predicts. Wave-solutions to reaction-diffusion equations with slowly decaying initial conditions can travel quite fast [9]. We conjecture that the wave profile in Figure 3 in [15] is unstable for the dynamic equation.

After some time, the fast moving, oscillating profile stops and develops into two objects: a slow-moving, non-monotone profile from zero to the unstable positive fixed point, and a plateau at that fixed point; see Figure 12. The oscillating pattern that developed initially appears relatively stationary. Different initial conditions lead to patterns that appear temporally constant and oscillate spatially between n_+ and n_- but differ in the spacing of the oscillations. These patterns therefore appear to be echoes of the initial condition.

For much larger times, either a secondary wave profile emerged, as observed in Figure 1 for example, or an oscillating pattern evolved that looked very much like the

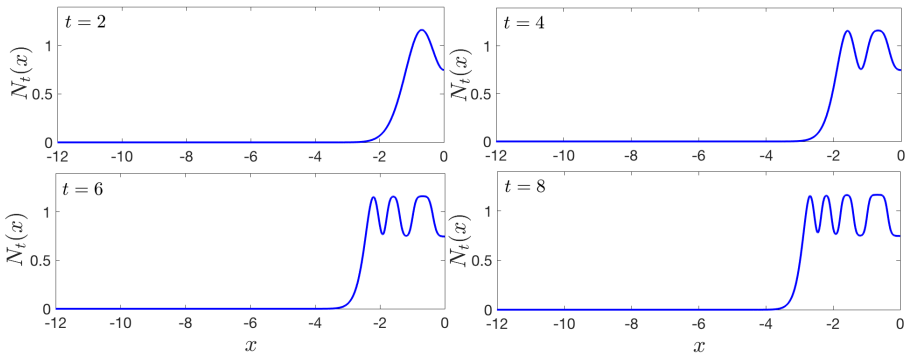

FIG. 11. *Short-time simulation of integrodifference equation (1) with scaled Gaussian initial condition* $N_0(x) = n_+ \exp(-x^2)$. *Only the region* $\{x < 0\}$ *is shown, the region* $\{x > 0\}$ *is symmetric. We used the logistic growth function and the Laplace dispersal kernel with parameters* $r = 2.2$ *and* $a = 50$, *respectively.*

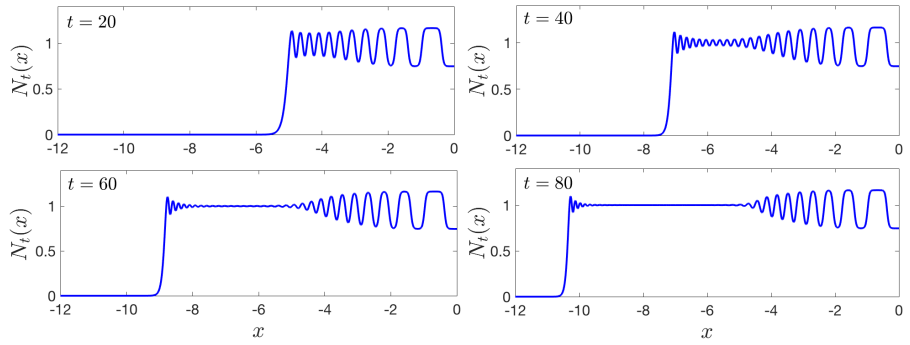

FIG. 12. *Intermediate-time simulation of (1) with scaled Gaussian initial condition* $N_0(x) = n_+ \exp(-x^2)$. *Only the region* $\{x < 0\}$ *is shown, the region* $\{x > 0\}$ *is symmetric. We used the logistic growth function and the Laplace dispersal kernel with parameters* $r = 2.2$ *and* $a = 50$, *respectively.*

second part of the profile from Figure 3 in [15], however, it was a standing-wave pattern, not a moving pattern. We tested these results with two independent numerical methods: Fast Fourier Transform (with which we had produced all previous simulation plots) or application of the trapezoidal rule to the convolution integral. In both cases, we observed what appeared to be instabilities after about 200 generations. More stable and more accurate numerical methods are necessary to explore the dynamic behaviour further. In particular, the question remains whether there are asymptotic patterns that are not spatially constant (i.e. at 1, n_+ or n_-). Since the bistable fronts between n_+ and n_- have speed zero (see previous section), it is conceivable that spatially oscillating, temporally stationary patterns could arise as concatenations of such transition fronts. Hence, the analytical challenge is to prove whether there are many coexisting, spatially oscillating steady-state patterns for the operator $\mathcal{S}$ (potentially a continuum) or whether this is a long-term transient phenomenon that will eventually be replaced by the simple, spatially homogeneous two-cycle.

Acknowledgments. FL thanks the participants of the workshop "Integrodifference equations in spatial ecology: 30 years and counting" (16w5121) at the Banff

International Research Station for their feedback on an oral presentation of this material.

REFERENCES

[1] M. Andersen, *Properties of some density-dependent integrodifference equation population models*, Mathematical Biosciences, 104 (1991), pp. 135–157.

[2] A. Bourgeois, *Spreading Speeds and Travelling Waves in Intergrodifference Equations with Overcompensatory Dynamics*, Master's thesis, University of Ottawa, https://www.ruor.uottawa.ca/handle/10393/34578, 2016.

[3] C. Cobbold, J. Roland, and M. Lewis, *The impact of parasitoid emergence time on host-parasitoid population dynamics*, Theoretical population biology, 75 (2009), pp. 201–215.

[4] R. Corless, G. Gonnet, D. Hare, D. Jeffrey, and D. Knuth, *On the Lambert W function*, Advances in Computational Mathematics, 5 (1996), pp. 329–359.

[5] R. Coutinho, W. Godoy, and R. Kraenkel, *Integrodifference model for blowfly invasion*, Theoretical Ecology, 5 (2012), pp. 363–371.

[6] J. Fang and X. Zhao, *Bistable traveling waves for monotone semiflows with applications*, Journal of European Mathematical Society, 17 (2015), pp. 2243–2288.

[7] P. Fife and J. McLeod, *The approach of solutions of nonlinear diffusion equations to travelling front solutions*, Archive for Rational Mechanics and Analysis, 65 (1977), pp. 335–361.

[8] A. Gharouni, M. Barbeau, A. Locke, L. Wang, and J. Watmough, *Sensitivity of invasion speed to dispersal and demography: an application of spreading speed theory to the green crab invasion on the northwest atlantic coast*, Marine Ecology Progress Series, 541 (2015), pp. 135–150.

[9] F. Hamel and L. Roques, *Fast propagation for kpp equations with slowly decaying initial conditions*, Journal of Differential Equations, 249 (2010), pp. 1726–1745.

[10] S. Hsu and X. Zhao, *Spreading speeds and traveling waves for nonmonotone integrodifference equations*, SIAM Journal on Mathematical Analysis, 40 (2008), pp. 776–789.

[11] M. Iida, R. Lui, and H. Ninomiya, *Stacked fronts for cooperative systems with equal diffusion coefficients*, SIAM Journal on Mathematical Analysis, 43 (2011), pp. 1369–1389.

[12] M. Kot, *Discrete-time traveling waves: Ecological examples*, Journal of Mathematical Biology, 30 (1992), pp. 413–436.

[13] M. Kot, M. Lewis, and P. van den Driessche, *Dispersal Data and the Spread of Invading Organisms*, Ecology, 77 (1996), pp. 2027–2042.

[14] M. Kot and W. Schaffer, *Discrete-time growth-dispersal models*, Mathematical Biosciences, 80 (1986), pp. 109–136.

[15] B. Li, M. Lewis, and H. Weinberger, *Existence of traveling waves for integral recursions with nonmonotone growth functions*, Journal of Mathematical Biology, 58 (2009), pp. 323–338.

[16] R. Lui, *Existence and stability of travelling wave solutions of a nonlinear integral operator*, Journal of Mathematical Biology, 16 (1983), pp. 199–220.

[17] F. Lutscher, R. Nisbet, and E. Pachepsky, *Population persistence in the face of advection*, Theoretical Ecology, 3 (2010), pp. 271–284.

[18] H. Malchow and S. Petrovskii, *Dynamical stabilization of an unstable equilibrium in chemical and biological systems*, Mathematical and Computer Modelling, 36 (2002), pp. 307–319.

[19] H. Malchow, S. Petrovskii, and E. Venturino, *Spatiotemporal Patterns in Ecology and Epidemiology*, Chapman and Hall CRC, 2008.

[20] N. Marculis and R. Lui, *Modelling the biological invasion of Carcinus maenas (the European green crab)*, Journal of Biological Dynamics, 10 (2016), pp. 140–163.

[21] R. May, *Biological populations obeying difference equations: Stable points, stable cycles, and chaos*, Journal of Theoretical Biology, 51 (1975), pp. 511–524.

[22] M. Neubert, M. Kot, and M. A. Lewis, *Dispersal and pattern formation in a discrete-time predator-prey model*, Theoretical Population Biology, 48 (1995), pp. 7–43.

[23] J. Powell, *Spatiotemporal models in ecology: an introduction to integro-difference equations*, tech. report, Utah State University, 2009.

[24] J. Roquejoffre, D. Terman, and V. Volpert, *Global stability of traveling fronts and convergence towards stacked families of waves in monotone parabolic systems*, SIAM Journal on Mathematical Analysis, 27 (1996), pp. 1261–1269.

[25] J. Sherratt, A. Dagbovie, and F. Hilker, *Mathematical biologists guide to absolute and convective instability*, Bulletin of Mathematical Biology, 76 (2014), pp. 1–26.

[26] O. Vasilyeva, F. Lutscher, and M. Lewis, *Analysis of spread and persistence for stream insects with winged adult stages*, Journal of Mathematical Biology, 72 (2016), pp. 851–875.

[27] M.-H. Wang and M. Kot, *Speeds of invasion in a model with strong or weak Allee effects*, Mathematical Biosciences, 171 (2001), pp. 83–97.
[28] M.-H. Wang, M. Kot, and M. Neubert, *Integrodifference equations, Allee effects and invasions*, Journal of Mathematical Biology, 44 (2002), pp. 150–168.
[29] H. Weinberger, *Asymptotic behavior of a model in population genetics*, Nonlinear partial differential equations and applications, 648 (1978), pp. 47–96.
[30] H. Weinberger, *Long-time behavior of a class of biological models*, SIAM Journal on Mathematical Analysis, 13 (1982), pp. 353–396.
[31] H. Weinberger and X.-Q. Zhao, *An extension of the formula for spreading speeds*, Mathematical Biosciences and Engineering, 7 (2010), pp. 187–194.
[32] T. Yi and X. Zou, *Asymptotic behavior, spreading speeds and traveling waves of nonmonotone dynamical systems*, SIAM Journal on Mathematical Analysis, 47 (2015), pp. 3005–3034.
[33] Z.-X. Yu and R. Yuan, *Properties of traveling waves for integrodifference equations with nonmonotone growth functions*, Zeitschrift fuer Angewandte Mathematik und Physik, 63 (2012), pp. 249–259.